Adsorption Science & Technology

Article

Adsorption of cationic dyes on activated carbon obtained from waste *Elaeagnus* stone

Adsorption Science & Technology
2016, Vol. 34(9–10) 512–525

DOI: 10.1177/0263617416669727
adt.sagepub.com
SAGE

Ünal Geçgel
Trakya University, Turkey

Osman Üner
Kırklareli University, Turkey

Güney Gökara
Trakya University, Turkey

Yüksel Bayrak
Trakya University, Turkey

Abstract

Activated carbon was obtained from waste *Elaeagnus* stone by a chemical activation method utilizing $ZnCl_2$. The resultant *Elaeagnus* activated carbon (EAC) with a high activated specific surface area of 1588 m^2/g was characterized using Brunauer–Emmett–Teller method, Fourier transform infrared spectra, point of zero charge, and scanning electron microscopy. The removals of cationic dyes, i.e., malachite green (MG), rhodamine B (RB), and methylene blue (MB) from aqueous solutions via EAC adsorption were characterized by investigating the effects of adsorbent concentration, contact time, initial dye concentration, and temperature. Langmuir model provided the most appropriate fit for all EAC dye adsorption processes, and the adsorption capacities for MB, RB, and MG at 25°C were calculated to be 288.18, 281.69, and 432.90 mg/g, respectively. The EAC adsorption curves of MB, RB, and MG follow a pseudo second-order kinetic model, and the calculated thermodynamic parameters, i.e., ΔG°, ΔH°, and ΔS° revealed that the synthetic dye adsorptions from aqueous solution were endothermic and spontaneous.

Keywords

Elaeagnus stone, methylene blue, rhodamine B, malachite green, activated carbon

Corresponding author:
Ünal Geçgel, Arda Vocational College, Trakya University, 22030 Edirne, Turkey.
Email: unalgecgel@trakya.edu.tr

Introduction

The widespread use of synthetic dyes in the dyeing and textile industries has resulted in severe problems to the health of humans and aquatic life worldwide because of the mutagenic, carcinogenic, or toxic properties of the dyes and their potentials to contaminate water resources (Karagozoglu et al., 2007). Thus, the efficient synthetic dye removals from aqueous solution have been a prominent concern. Various chemical, physical, and biological methods for dye removal have been developed (Srinivasan and Viraraghavan, 2010). One of these methods is adsorption, which is an advantageous technique because of its simplicity of design, availability of adsorbents, and low cost. In recent adsorption experiments for the removal of pollutants, various types of adsorbents have been investigated, and activated carbon, obtained from waste biomaterials through physical and chemical activation methods, has become a popular adsorbent (Yagub et al., 2014a). Chemical agents such as $ZnCl_2$, H_3PO_4, H_2SO_4, K_2S, KCNS, HNO_3, H_2O_2, $KMnO_4$, $(NH_4)_2S_2O_8$, NaOH, KOH, and K_2CO_3 are used to activate the carbons for adsorption—a process referred to as chemical activation (Yahya et al., 2015). Among these chemical activating agents, $ZnCl_2$ is widely preferred because it is efficient in producing the desired microporous structure and a greater surface area (Donald et al., 2011).

Elaeagnus stone, a waste biomaterial, has not sufficiently been studied as a starting material in producing activated carbon. Therefore, in this paper, *Elaeagnus* stone was used, and it was chemically activated using $ZnCl_2$ to produce an activated carbon with high surface area. Also, the adsorption performance of the obtained *Elaeagnus* activated carbon (EAC) was examined for three cationic dyes, i.e., malachite green (MG), methylene blue (MB), and rhodamine B (RB). The performances of EAC on dye adsorptions were evaluated using equilibrium, kinetic, and thermodynamic studies.

Materials and methods

Materials

The *Elaeagnus* stones were obtained from trees in Edirne, Turkey. After *Elaeagnus* stones were cleaned using double-distilled water, they were stayed at room temperature for about seven days to dry their water. Then, they were ground to have particles smaller than 50 mesh, and placed into brown bottles for future use. The adsorbates MB ($C_{16}H_{18}N_3ClS$ whose molecular weight is 319.85 g/mol), MG ($C_{23}H_{25}ClN_2$ whose molecular weight is 364.911 g/mol), and RB ($C_{28}H_{31}ClN_2O_3$ whose molecular weight is 479.020 g/mol) were provided by Merck. Dye stock solutions were prepared at 1000 mg/L concentrations by dissolving dye powders at required amounts in distilled water. By diluting the dye stock solutions with distilled water, the solutions at required concentration were adjusted for adsorption experiments. $ZnCl_2$ was supplied from Merck.

Preparing activated carbon and determining optimal $ZnCl_2$ concentration

Ten grams of milled *Elaeagnus* stone was inserted into each of the flasks, and 20%, 30%, and 40% (w/w) $ZnCl_2$ solutions were mixed with these *Elaeagnus* stones to activate the carbons, separately. The mixtures in the flasks were heated under reflux just below their boiling points (around 90°C) for 60 min and then dried in petri dishes in an incubator for 24 h at 105°C. After drying, the carbonization of the *Elaeagnus* stone was completed by baking at 600°C for 60 min. The produced EACs were soaked in 0.1 N HCl solutions and stirred in order to remove zinc and chloride compounds and also contaminants on surfaces. Then, they were

washed with double-distilled water till pH reached to neutral. Last, in the incubator at 105°C, an additional drying step was completed before the EACs were ground and stored for future use. The optimal $ZnCl_2$ concentration for the preparation of high specific surface area EACs was determined by measuring the obtained EAC specific surface areas.

Characterization of prepared EAC

Nitrogen (N_2) adsorption–desorption experiments were performed at liquid nitrogen temperature (−196.15°C) by means of Micromeritics TriStar II 3020. To remove volatile contaminations, degassing processes were completed for EACs at 90°C for 0.5 h and immediately after, at 300°C for 2 h under vacuum before measurements. By using the Brunauer–Emmett–Teller (BET) method, specific surface areas were determined, and total pore volumes were calculated through nitrogen adsorption at $P/P_0 = 0.984$. Surface functional groups were determined by Fourier transform infrared spectra (FTIR; FAR-FT-IR Perkin Elmer). Furthermore, the pH_{pzc} was measured as follows: 50 mL of KNO_3 solution (0.1 M) was placed in an Erlenmeyer flask including 0.1 g of EAC. The initial pH was adjusted between 2 and 11 by addition of NaOH or HCl (0.1 N). After a contact time of 48 h under magnetic agitation, the ultimate pH was determined and plotted versus the initial pH (Milonjić et al., 1975). Also, EAC surface features were investigated using scanning electron microscopy (SEM; FEI-QUANTA FEG 250).

Adsorption experiments

The adsorption experiments were performed with batch method. In batch adsorption studies, the dye solutions at the desired concentrations were adjusted from dye stock solutions through dilution with water, and placed in Erlenmeyer flasks. After that, EACs were put in the Erlenmeyer flasks. They were located into a shaker with thermostat-controlled (WiseBath) and shaken at 150 r/min till adsorption equilibrium was reached at desired temperature. Samples were then centrifuged for 20 min at 4000 r/min to set apart their solid phases from liquid phases, and their remaining dye amounts without adsorbed in solutions were detected using a UV–visible spectrophotometry (Mecasys Optizen POP Series) at 665, 620, and 555 nm wavelengths for MB, MG, and RB, respectively. Using the above method, adsorption experiments were performed to assess the effects of EAC concentration (0.0125–0.125 g/50 mL), initial dye concentration (200–500 mg/L), and temperature (25°C–45°C). Adsorbed dye amount per unit mass of EAC (q_e) was calculated via the equation:

$$q_e = \frac{(C_i - C_e)V}{\mathrm{W}} \tag{1}$$

The formula below provides to calculate the percentage of the dye removed:

$$Removal\,(\%) = \frac{(C_i - C_e)}{C_i} \times 100 \tag{2}$$

where w is the mass of the adsorbent (g), V is the volume of the solution (L), C_e is the equilibrium concentration of the dye solution (mg/L), and C_i is the initial dye concentration (mg/L).

Table 1. Characteristics of EAC.

$ZnCl_2$ concentration (w/w%)	20	30	40
BET Surface area (m^2/g)	1121	1588	1404
Micropore area (m^2/g)	350.75	1139.37	903.49
Total pore volume (cm^3/g)	0.57	0.90	0.97
Micropore volume (cm^3/g)	0.22	0.08	0.01
Average pore diameter (nm)	2.04	2.27	2.77

BET: Brunauer–Emmett–Teller; EAC: *Elaeagnus* activated carbon.

Results and discussion

EAC characteristics

The characteristics of EAC are listed in Table 1. When a 30% (w/w) $ZnCl_2$ solution was used during the chemical activation process, EAC with a considerably high specific surface area of 1588 m^2/g was obtained. Furthermore, the micropore volume, total pore volume, micropore area, BET specific surface area, and average pore diameter show that the synthesized EAC has a suitably porous surface for the adsorption of dye molecules. The total pore volumes were obtained at a relative pressure of about 0.98, and micropore surface areas and micropore volumes were estimated using t-plot method (Lowell and Shields, 1991). The infrared spectra of *Elaeagnus* stone and EAC are displayed in Figure 1 (a) to (b). In raw material FTIR spectrum, the broad absorption band between 3200 and 3400 cm^{-1} shows the existences of OH groups and the vibration of N–H stretching (Dağdelen et al., 2014). The bands located at 2923 and 2854 cm^{-1} indicate C–H vibrations methylene and methyl groups (Sun and Webley, 2010). The band at 1744 cm^{-1} indicates carbonyl C=O groups. The band located at 1614 cm^{-1} correspond to olefinic C=C stretching (Yu and Luo 2014). The two bands at 1541 and 1456 cm^{-1} indicate the skeletal C=C vibrations in aromatic rings and the bands at around 1445 and 1376 cm^{-1} is due to the C–H in-plane bending vibrations in methyl and methylene groups (Yang and Qiu, 2010). The bands located at 1239 cm^{-1} and an intense band at approximately 1027 cm^{-1} belongs to C–O stretching vibrations in alcohols, phenols, or ether or ester groups (Hesas et al., 2013). EAC spectrum has less adsorption bands than the raw material spectrum. This indicates that various functional groups present in raw material spectrum disappeared after the carbonization and activation steps. Similar to the raw material spectrum, the bands between 1154 and 1035 cm^{-1} are attributed to C–O stretching in carboxyl acids, alcohols, phenols, and esters (Martins et al., 2015). The value at which pH (ultimate) was equal to pH (initial) was accepted to be pH_{PZC}, and the charge surface is neutral at this pH value. The pH_{PZC} of an adsorbent is a fundamental characteristic to comprehend interfacial properties, and the value of pH_{PZC} of EAC was determined to be 7.05 as shown in supplementary file. Surface texture, fundamental physical properties, and pore morphology of the adsorbent surface were characterized using SEM. Figure 2(a) to (b) displays the SEM images of EAC surfaces with an impregnation ratio of 30% (w/w). A dissimilar texture with rough cavities and many holes were observed on EAC surfaces. Considering the results of the BET method and SEM analysis, EAC was determined to have an appropriate structure for the adsorption processes of dye molecules.

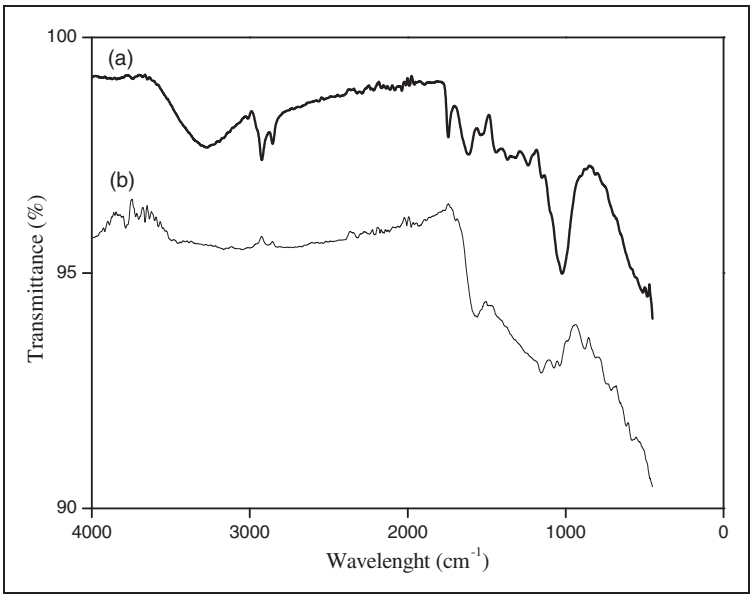

Figure 1. FTIR images of *Elaeagnus* stone (a) and *Elaeagnus* activated carbon (b). FTIR: Fourier transform infrared spectra.

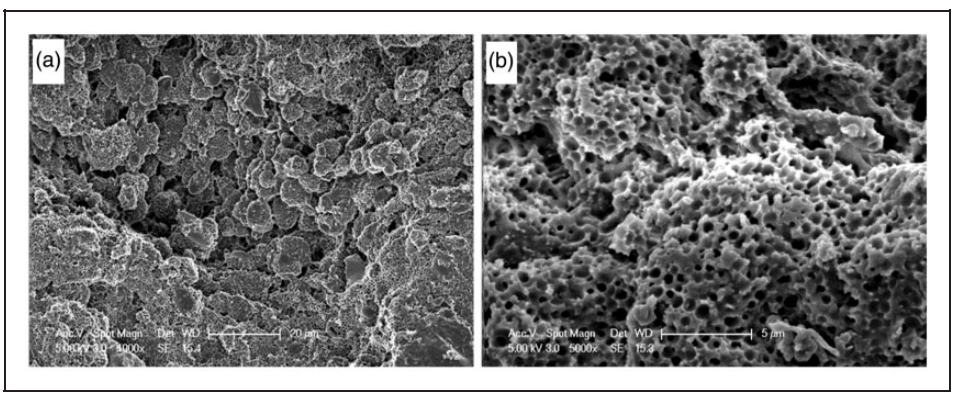

Figure 2. SEM images of EAC activated with 30% (w/w) $ZnCl_2$ (a) 1000× and (b) 5000×.
EAC: *Elaeagnus* activated carbon; SEM: scanning electron microscopy.

Effect of adsorbent concentration

In Figure 3, the effect of adsorbent concentration on dye removal efficiency is displayed for the cationic dyes (i.e., MB, MG, and RB). The removal efficiencies of dyes increased when the amount of EAC increased, as the number of the active sites to which the dye molecules could bind increased. The optimal adsorbent concentrations were found to be 1 g/L for MB

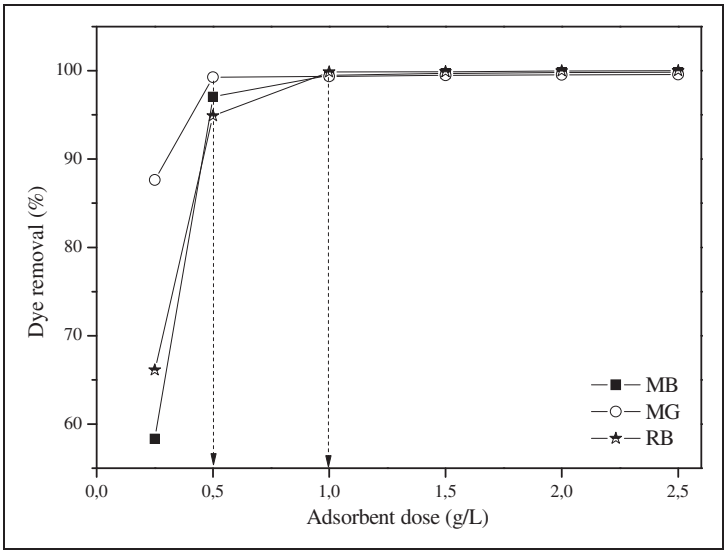

Figure 3. Effect of adsorbent concentration on the percentage of dye removal (initial dye concentration = 200 mg/L, contact time = 75 min, agitation rate = 150 r/min, temperature = 25°C, pH = 7).

as well as RB and the optimal adsorbent concentration was determined to be 0.5 g/L for MG. Also, 99.50% dye removal was attained using 1 g/L of EAC.

The optimal adsorbent concentration for MG removal is substantially lower than literature values for MB (Ghaedi et al., 2014b; Li et al., 2011), MG (Dahri et al., 2014; Ghaedi et al., 2014a), and RB (Lacerda et al., 2015) for various other adsorbents.

Effect of initial dye concentration and contact time

Figure 4 (a) to (c) illustrates the effect of initial dye concentration and contact time on the removal of MB, MG, and RB, respectively, from aqueous solutions. In this figure, similar trends are observed for all the cationic dyes. That is, while the increase in contact time has a positive effect, the increase in initial dye concentration adversely affects the EAC dye removal. When initial dye concentrations were increased from 200 to 500 mg/L, the dye removal decreased from 96.50% to 61.35%, from 99.02% to 81.65%, and from 96.10% to 61.06% for MB, MG, and RB, respectively. Moreover, the time needed to attain equilibrium increased with the increase in dye concentration. For instance, for the 200 mg/L initial dye concentration, equilibrium was attained in 75, 30, and 60 min, whereas for the 500 mg/L initial dye concentration, equilibrium was attained after 155, 145, and 180 min for MB, MG, and RB, respectively. Thus, the increase in the initial dye concentration increased the electrostatic repulsion forces between the dye molecules in solution and the dye molecules adsorbed by EAC.

Effect of temperature

Six different dye concentrations (200–500 mg/L) at different temperatures (25°C, 35°C, and 45°C) were used to examine the effect of temperature on the removal of dyes from aqueous solutions. For each dye, the effects of initial dye concentration and temperature are

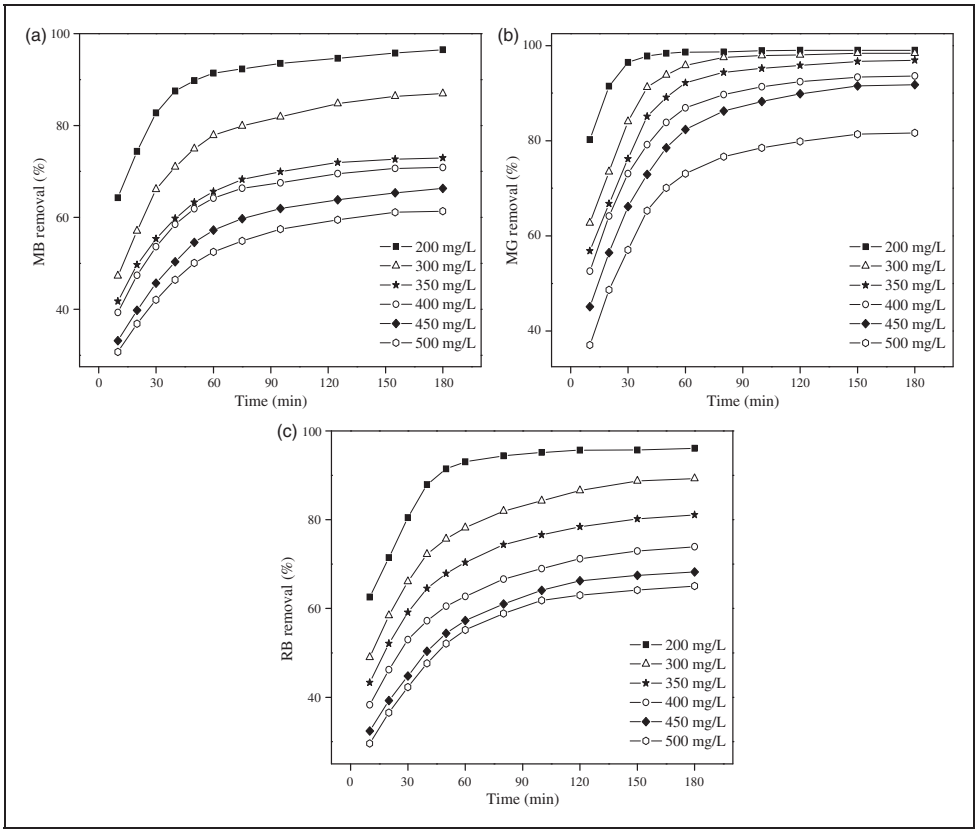

Figure 4. Effect of contact time and initial concentration on the percentages of MB (a), MG (b), and RB (c) removals (agitation rate = 150 r/min, temperature = 25°C, pH = 7, and adsorbent concentration = 1 g/L). MB: methylene blue; MG: malachite green; RB: rhodamine B.

presented in Figure 5. From this figure, an increase in temperature increased the adsorption of MB, MG, and RB on EAC. Because of the high adsorption capacity of EAC, dye removal from the aqueous solutions only increased slightly with increasing temperature at low dye concentrations ($C_i \leq 300$ mg/L), such as from 96.5% to 98.74%, from 99.76% to 99.83%, and from 98.96% to 99.19% for MB, MG, and RB solutions, respectively, with an initial concentration of 200 mg/L. However, dye removal substantially increased at higher temperatures for higher initial dye concentrations ($C_i > 300$ mg/L), such as from 56.29% to 63.85%, from 85.98% to 98.14%, and from 57.26% to 77.80% for MB, MG, and RB solutions, respectively, with an initial concentration of 500 mg/L. These results indicate that MB, MG, and RB adsorption by EAC is an endothermic process.

Equilibrium studies

The adsorption isotherms are important tools to understand the distribution of adsorbate molecules among the solid and liquid phases at equilibrium. Furthermore, adsorption isotherms describe the adsorbate interaction with the adsorbent, including the adsorption

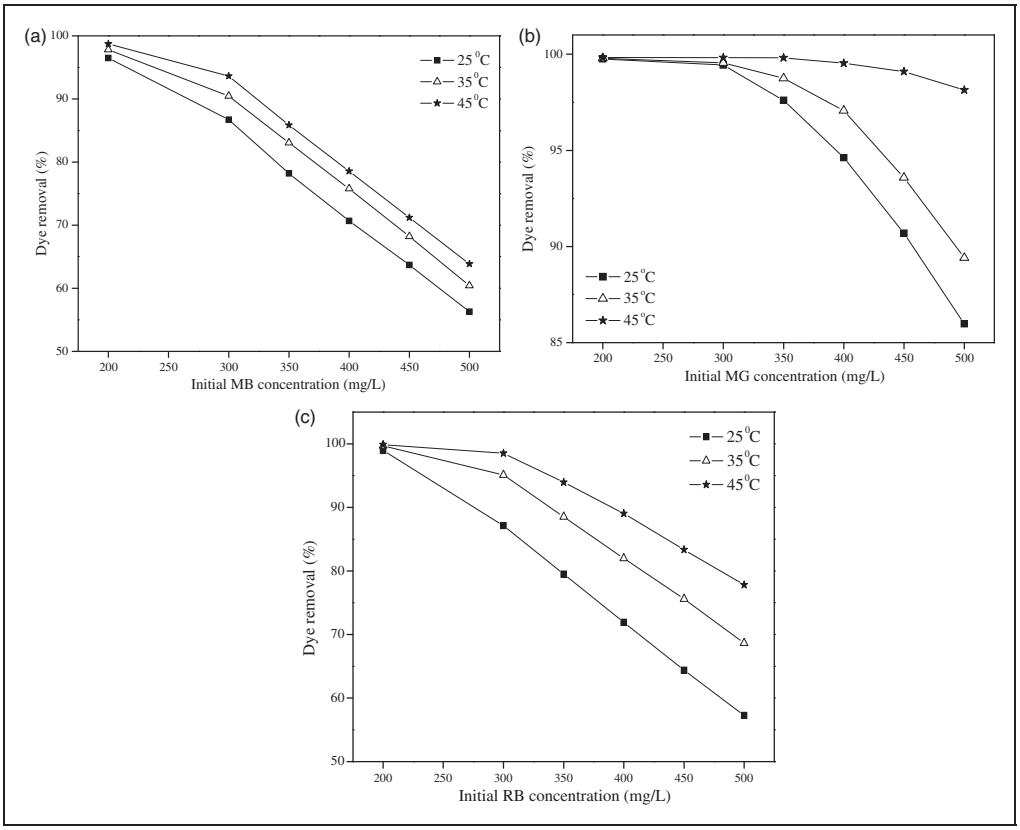

Figure 5. Effect of temperature on the percentages of MB (a), MG (b), and RB (c) removals for different initial dye concentrations (agitation rate = 150 r/min, pH = 7, and adsorbent concentration = 1 g/L). MB: methylene blue; MG: malachite green; RB: rhodamine B.

features and types. The fitting of data is accomplished using diverse models in order to design adsorption systems (Dağdelen et al., 2014). For this aim, Langmuir (1916) and Freundlich (1906) models were performed to the adsorption data of MB, MG, and RB on EAC.

Langmuir model presumes constant adsorption energy and independent of surface coverage. When a monolayer of adsorbate covers the adsorption surface, maximum adsorption is observed. The following equation below is Langmuir isotherm equation.

$$\frac{C_e}{q_e} = \frac{1}{q_m K_L} + \frac{C_e}{q_m} \tag{3}$$

where K_L is Langmuir adsorption constant (L/mg) and q_m is the complete monolayer adsorption capacity (mg/g). Separation factor R_L can identify the favorability of the adsorption process (Hall et al., 1966), which is calculated through the following formula:

$$R_L = \frac{1}{1 + K_L C_i} \tag{4}$$

Table 2. Adsorption isotherm parameters for the adsorption of MB, MG, and RB onto EAC.

Adsorption isotherm models and their constants	Temperature (K)								
	298			308			318		
Dyes	MB	RB	MG	MB	RB	MG	MB	RB	MG
Langmuir									
q_m (mg/g)	288.18	281.69	432.90	308.64	349.65	452.49	324.67	389.10	512.82
K_L (L/mg)	0.2880	0.2584	0.6078	0.3418	0.3210	0.8308	0.3765	0.4283	2.1891
R^2	0.9998	0.9983	0.9991	0.9998	0.9988	0.9994	0.9999	0.9990	0.9995
R_L	0.017	0.019	0.008	0.014	0.015	0.006	0.013	0.011	0.002
Freundlich									
K_F (mg/g) (L/mg)$^{1/n}$	160.88	191.28	245.34	171.72	213.14	256.45	186.71	239.61	318.32
$1/n$	0.11484	0.07285	0.14059	0.11910	0.09973	0.15474	0.11387	0.10423	0.22549
R^2	0.95498	0.96019	0.96445	0.95994	0.98613	0.95984	0.96435	0.99244	0.90519

EAC: *Elaeagnus* activated carbon; MB: methylene blue; MG: malachite green; RB: rhodamine B.

where R_L values give significant information about adsorption, which are $R_L = 1$ for linear adsorption, $R_L = 0$ for irreversible adsorption, $0 < R_L < 1$ for favorable adsorption, and $R_L > 1$ for unfavorable adsorption. According to the Freundlich model, adsorption takes place on the heterogeneous surfaces of varied affinities. The following equation is the linear form of the Freundlich model:

$$\ln q_e = \ln K_F + \frac{1}{n} \ln C_e \tag{5}$$

where K_F is the Freundlich adsorption constant ((mg/g) (L/mg)$^{1/n}$) and n (dimensionless) is the empirical parameter about the adsorption intensity, which alters with the heterogeneity of material. If the values of $1/n$ are between 0 and 1, it is considered to be favorable adsorption on a surface.

At three different temperatures (25°C, 35°C, and 45°C), Langmuir and Freundlich adsorption isotherms were drawn as seen in supplementary file to examine the binding mechanisms of MB, MG, and RB adsorptions on EAC. The Langmuir and Freundlich adsorption isotherm constants were calculated at three temperatures, and they are listed in Table 2. When assessing the values of the correlation coefficients (R^2) for both models, the correlations of the Freundlich model were lower than those obtained from Langmuir model at three adsorption temperature (Table 2). Therefore, the adsorption equilibria of MG, MB, and RB on EAC are more well fitted with the Langmuir model than the Freundlich model, which suggests that MB, MG, and RB molecules cover the EAC surface as a monolayer onto the characteristic homogeneous sites. Furthermore, the R_L and $1/n$ constants are between 0 and 1 at all temperatures, expressing that they are favorable for the adsorptions of MB, MG, and RB on EAC. When compared with the adsorption capacities of MB (Mahmoudi et al., 2015; Theydan and Ahmed, 2012; Yagub et al., 2014b), MG (Dahri et al., 2014; Ghaedi et al., 2014a; Kan et al., 2015), and RB (Lacerda et al., 2015; Li et al., 2010; Liu et al., 2015) on various adsorbents in previous studies, EAC is seen to be an effective adsorbent for MB, MG, and RB in aqueous solution.

Using the PCMODEL program with an MMX force field, the molecular volumes for MB, MG, and RB were calculated as 371.07, 475.80, and 581.97 $Å^3$, respectively. From these calculated molecular volumes, the adsorption capacity of EAC was expected to be MB > MG > RB; however, the adsorption capacity was experimentally determined to be MG > MB > RB. This contradiction can be explained by the resonance form of MB. MB has a positive charge on its S atom due to its resonance form; thus, the positively charged S atom binds to the EAC surface. Therefore, MB molecules occupy larger areas on the EAC surface, sterically hindering the binding of additional MB molecules. MG molecules occupy less area on the EAC surface than the MB molecules by binding with positively charged N atoms, allowing for the binding of additional MG molecules on the EAC surface. The interactions (probably electrostatic interactions and π–π stacking) of dye functional groups with the EAC surface (C–O stretching in carboxyl acids, alcohols, phenols, and esters determined from FTIR spectrum) explain that the adsorption of MG is higher than the adsorption of MB on EAC. EAC has the smallest adsorption capacity for RB because of RB's larger molecular volume.

Kinetic studies

Pseudo first-order and pseudo second-order models were performed to the adsorption of dyes on EAC. The pseudo first-order equation (Lagergren, 1898) is given by the following equation.

$$\log(q_e - q_t) = \log q_e - \frac{k_1 t}{2.303} \tag{6}$$

The pseudo second-order equation (Ho and McKay, 1999) is given by

$$\frac{t}{q_t} = \frac{1}{k_2 q_e^2} + \frac{1}{q_e} t \tag{7}$$

where k_1 and k_2 symbolize the pseudo first-order and pseudo second-order rate constants, respectively. q_t (mg/g) is the amount of dye adsorbed on EAC at time t. In addition to R^2, the normalized standard deviations (Δq_e) were calculated using the following equation to determine the most appropriate kinetic model for MB, MG, and RB adsorptions on EAC.

$$\Delta q_e(\%) = \sqrt{\frac{\sum_{i=1}^{N} \left(\frac{q_{e,exp} - q_{e,cal}}{q_{e.exp}} \right)^2}{N - 1}} \times 100 \tag{8}$$

In the formula above, N represents the number of experimental data points.

For MB, MG, and RB adsorptions on EAC, Table 3 shows the parameters for pseudo first-order and pseudo second-order kinetic models with initial dye concentrations of 200–500 mg/L. Table 4 presents the normalized standard deviations of MB, MG, and RB adsorption on EAC for pseudo first-order and pseudo second-order kinetic models.

The pseudo second-order kinetic model had a much better correlation fit for the dye adsorption data than the pseudo first-order model for all dyes and all initial

Table 3. Comparison of the pseudo first-order and pseudo second-order adsorption rate constants at different initial MB, MG, and RB concentrations.

			Pseudo first-order model			Pseudo second-order model		
Initial dye concentration (mg/L)	Dyes	q_{exp} (mg/g)	$q_{e\ cal.}$ (mg/g)	k_1 (1/min)	R^2	$q_{e,\ cal.}$ (mg/g)	k_2 (g/mg min)	R^2
200	MB	192.990	58.100	0.0241	0.982	198.413	0.000875	1.000
	RB	192.200	70.786	0.0345	0.977	201.207	0.000799	1.000
	MG	198.041	88.990	0.0497	0.939	202.429	0.000297	1.000
300	MB	260.850	150.668	0.0270	0.992	277.778	0.000310	1.000
	RB	267.750	132.391	0.0215	0.989	280.900	0.000311	1.000
	MG	295.113	242.789	0.0569	0.966	309.597	0.000533	1.000
350	MB	255.325	162.705	0.0315	0.997	272.480	0.000333	1.000
	RB	283.850	169.145	0.0252	0.996	303.030	0.000254	0.999
	MG	339.290	177.439	0.0344	0.992	361.011	0.000314	0.999
400	MB	283.519	184.646	0.0315	0.985	303.030	0.000297	1.000
	RB	295.600	170.962	0.0225	0.998	316.456	0.000218	0.999
	MG	374.560	226.678	0.0335	0.996	400.000	0.000247	1.000
450	MB	298.347	184.633	0.0237	0.998	322.581	0.000204	0.999
	RB	306.990	239.067	0.0272	0.995	340.136	0.000161	0.999
	MG	412.920	339.453	0.0343	0.983	452.489	0.000156	1.000
500	MB	306.748	184.633	0.0237	0.999	374.532	0.000126	0.979
	RB	325.300	243.545	0.0265	0.999	362.319	0.000147	1.000
	MG	408.254	327.997	0.0331	0.989	450.450	0.000145	0.999

MB: methylene blue; MG: malachite green; RB: rhodamine B.

Table 4. The values of the normalized standard deviations (Δq_e).

Dyes	Pseudo first-order model Δq (%)	Pseudo second-order model Δq (%)
MB	49.47	11.80
RB	47.07	8.80
MG	39.71	6.68

MB: methylene blue; MG: malachite green; RB: rhodamine B.

dye concentrations (Table 3). Moreover, the normalized standard deviations, shown in Table 4, suggest that the pseudo second-order kinetic model fits well for MG, MB, and RB adsorption on EAC.

Thermodynamic studies

Using the following equations, the thermodynamic parameters, which are standard free energy change (ΔG°), enthalpy (ΔH°), and entropy (ΔS°), were obtained to examine the

Table 5. Thermodynamic parameters for MB, MG, and RB adsorptions onto EAC.

	Temperature (K)	ΔG° (kJ/mol)	ΔH° (kJ/mol)	ΔS° (kJ/mol K)	R^2
MB	298	−28.774			
	308	−30.093	10.552	0.1319	0.989
	318	−31.412			
RB	298	−29.026			
	308	−30.667	19.900	0.1641	0.995
	318	−32.308			
MG	298	−30.831			
	308	−33.550	50.236	0.2719	0.953
	318	−36.269			

EAC: *Elaeagnus* activated carbon; MB: methylene blue; MG: malachite green; RB: rhodamine B.

dye adsorptions on EAC thermodynamically.

$$\Delta G^\circ = -RTlnK_d \tag{9}$$

$$\Delta G^\circ = \Delta H^\circ - T\Delta S^\circ \tag{10}$$

$$\ln K_d = \frac{-\Delta H^\circ}{R}\frac{1}{T} + \frac{\Delta S^\circ}{R} \tag{11}$$

where, R is the universal gas constant (8.314 J/mol K), T is the absolute temperature in Kelvin, and K_d is the equilibrium constant obtained from Langmuir constant K_L (Liu, 2006). By drawing the van't Hoff plot of $ln\ K_d$ versus $1/T$, the ΔH° and ΔS° values were found from the slope and intercept. Table 5 lists the ΔH°, ΔS°, and ΔG° values at various temperatures for MB, MG, and RB adsorption on EAC.

When assessing the obtained thermodynamic parameters, negative ΔG° values reveal that MB, MG, and RB adsorption on EAC is spontaneous. Moreover, the positive values of ΔS° show that an increase occurs in the randomness in the system of the solid/solution interface during the adsorption process. The fact that ΔH° values are positive reconfirm that the adsorption of MB, MG, and RB is endothermic.

Conclusions

Using chemical activation with $ZnCl_2$, activated carbon was obtained from waste *Elaeagnus* stone. The functional groups on the activated carbon obtained were determined as C–O stretching in carboxyl acids, alcohols, phenols, and esters through FTIR spectrum, and the pH_{pzc} was found to be 7.05. This activated carbon has a high adsorption capacity for the removal of cationic dyes, i.e., MB, RB, and MG, from aqueous solutions. It was determined that the adsorbent's adsorption capacity was dependent on both the molecular volume of the dyes and their chemical structures, especially their functional groups. At high initial dye concentrations, an increase in temperature led to a significant increase in the adsorption efficiency of all three dyes on EAC. Even at low adsorbent concentrations, more than 99.50% of the dyes were removed from the solution. Equilibrium data for the cationic

dyes/EAC systems were well fitted to Langmuir isotherms, and the rates of adsorptions were determined to follow the pseudo second-order kinetic model. Negative ΔG° values indicated that the adsorption of MB, MG, and RB on EAC was spontaneous. Positive ΔH° values proved the endothermic nature of the adsorption of all the dyes. Consequently, activated carbon obtained from waste *Elaeagnus* stone has been figured out to be an effective and low-cost adsorbent for the removal of synthetic cationic dyes from aqueous solutions.

Declaration of Conflicting Interests

The author(s) declared no potential conflicts of interests with respect to the research, authorship, and/or publication of this article.

Funding

The author(s) received no financial support for the research, authorship, and/or publication of this article.

Supplemental Material

The online supplementary file is available at http://adt.sagepub.com/supplemental.

References

Dağdelen S, Acemioğlu B, Baran E, et al. (2014) Removal of remazol brilliant blue R from aqueous solution by pirina pretreated with nitric acid and commercial activated carbon. *Water Air Soil Pollution* 225: 1–15.

Dahri MK, Kooh MRR and Lim LBL (2014) Water remediation using low cost adsorbent walnut shell for removal of malachite green: Equilibrium, kinetics, thermodynamics and regeneration studies. *Journal of Environmental Chemical Engineering* 2: 1434–1444.

Donald J, Ohtsuka Y and Xu CC (2011) Effects of activation agents and intrinsic minerals on pore development in activated carbons derived from a Canadian peat. *Materials Letters* 65: 744–747.

Freundlich HMF (1906) Über die adsorption in lösungen. *Zeitschrift fur Physikalische, Chemie* 57: 385–470.

Ghaedi M, Ansari A, Habibi MH, et al. (2014a) Removal of malachite green from aqueous solution by zinc oxide nanoparticle loaded on activated carbon: Kinetics and isotherm study. *Journal of Industrial and Engineering Chemistry* 20: 17–28.

Ghaedi M, Nasab AG, Khodadoust S, et al. (2014b) Application of activated carbon as adsorbents for efficient removal of methylene blue: Kinetics and equilibrium studies. Journal of Industrial and Engineering Chemistry 20: 2317–2324.

Hall KR, Eagleton LC, Acrivos A, et al. (1966) Pore- and solid-diffusion kinetics in fixed-bed adsorption under constant-pattern conditions. *Industrial and Engineering Chemistry Fundamentals* 5: 212–223.

Hesas RH, Niya AA, Daud WMAW, et al. (2013) Preparation of granular activated carbon from oil palm shell by microwave-induced chemical activation: Optimization using surface response methodology. *Chemical Engineering Research and Design* 91: 2447–2456.

Ho YS and McKay G (1999) Pseudo-second order model for sorption processes. *Process Biochemistry* 34: 451–465.

Kan Y, Yue Q, Kong J, et al. (2015) The application of activated carbon produced from waste printed circuit boards (PCBs) by H_3PO_4 and steam activation for the removal of malachite green. *Chemical Engineering Journal* 260: 541–549.

Karagozoglu B, Tasdemir M, Demirbas E, et al. (2007) The adsorption of basic dye (Astrazon Blue FGRL) from aqueous solutions onto sepiolite, fly ash and apricot shell activated carbon: Kinetic and equilibrium studies. *Journal of Hazardous Material* 147: 297–306.

Lacerda VDS, Lopez-Sotelo JB, Correa-Guimaraes A, et al. (2015) Rhodamine B removal with activated carbons obtained from lignocellulosic waste. *Journal of Environmental Management* 155: 67–76.

Lagergren S (1898) Zur theorie der sogenannten adsorption gelöster stoffe. *Kungliga Svenska Vetenskapsakademiens Handlingar* 24: 1–39.

Langmuir I (1916) The constitution and fundamental properties of solids and liquids. *Journal of American Chemical Society* 38: 2221–2295.

Li L, Liu S and Zhu T (2010) Application of activated carbon derived from scrap tires for adsorption of Rhodamine B. *Journal of Environmental Sciences* 22: 1273–1280.

Li W-H, Yue Q-Y, Gao B-Y, et al. (2011) Preparation and utilization of sludge-based activated carbon for the adsorption of dyes from aqueous solutions. *Chemical Engineering Journal* 171: 320–327.

Liu K, Li H, Wang Y, et al. (2015) Adsorption and removal of rhodamine B from aqueous solution by tannic acid functionalized graphene. *Colloids and Surfaces A: Physicochemical Engineering Aspects* 477: 35–41.

Liu Y (2006) Some consideration on the Langmuir isotherm equation. *Colloids and Surfaces A: Physicochemical and Engineering Aspects* 274: 34–36.

Lowell S and Shields JE (1991) *Powder Surface Area and Porosity* 3rd ed. London: Chapman & Hall.

Mahmoudi K, Hosni K, Hamdi N, et al. (2015) Kinetics and equilibrium studies on removal of methylene blue and methyl orange by adsorption onto activated carbon prepared from date pits—A comparative study. *Korean Journal of Chemical Engineering* 32: 274–283.

Martins AC, Pezoti O, Cazetta AL, et al. (2015) Removal of tetracycline by NaOH-activated carbon produced from macadamia nut shells: Kinetic and equilibrium studies. *Chemical Engineering Journal* 260: 291–299.

Milonjić SK, Ruvarac AL and Šušić MV (1975) The heat of immersion of natural magnetite in aqueous solutions. *Thermochimica Acta* 11: 261–266.

Srinivasan A and Viraraghavan T (2010) Decolorization of dye wastewaters by biosorbents: A review. *Journal of Environmental Management* 91: 1915–1929.

Sun Y and Webley PA (2010) Preparation of activated carbons from corncob with large specific surface area by a variety of chemical activators and their application in gas storage. *Chemical Engineering Journal* 162: 883–892.

Theydan SK and Ahmed MJ (2012) Adsorption of methylene blue onto biomass-based activated carbon by $FeCl_3$ activation: Equilibrium, kinetics, and thermodynamic studies. *Journal of Analytical and Applied Pyrolysis* 97: 116–122.

Yagub MT, Sen TK, Afroze S, et al. (2014a) Dyes and its removal from aqueous solution by adsorption: A review. *Advances in Colloid and Interface Science* 209: 172–184.

Yagub MT, Sen TK and Ang M (2014b) Removal of cationic dye methylene blue (MB) from aqueous solution by ground raw and base modified pine cone powder. *Environmental Earth Science* 71: 1507–1519.

Yahya MA, Al-Qodah Z and Zanariah Ngah CW (2015) Agricultural bio-waste materials as potential sustainable precursors used for activated carbon production: A review. *Renewable and Sustainable Energy Reviews* 46: 218–235.

Yang J and Qiu K (2010) Preparation of activated carbon from walnut shell via vacuum chemical activation and their application for methylene blue removal. *Chemical Engineering Journal* 165: 209–217.

Yu L and Luo Y-M (2014) The adsorption mechanism of anionic and cationic dyes by Jerusalem artichoke stalk-based mesoporous activated carbon. *Journal of Environmental Chemical Engineering* 2: 220–229.